SIAM J. SCI. COMPUT.
Vol. 37, No. 1, pp. A369–A390
© 2015 Society for Industrial and Applied Mathematics

THE MULTISYMPLECTIC DIAMOND SCHEME*

R. I. MCLACHLAN† AND M. C. WILKINS†

Abstract. We introduce a class of general purpose linear multisymplectic integrators for Hamiltonian wave equations based on a diamond-shaped mesh. On each diamond, the PDE is discretized by a symplectic Runge–Kutta method. The scheme advances in time by filling in each diamond locally, leading to greater efficiency and parallelization and easier treatment of boundary conditions compared to methods based on rectangular meshes.

Key words. multisympletic integrators, multi-Hamiltonian PDE, finite difference methods, geometric numerical integration

AMS subject classifications. 37M15, 37K05, 65P10

DOI. 10.1137/140958359

1. Introduction.

In this paper we consider multisymplectic integrators for the class of multi-Hamiltonian PDEs

$$K\mathbf{z}_t + L\mathbf{z}_x = \nabla S(\mathbf{z}), \tag{1.1}$$

where K and L are constant $n \times n$ real skew-symmetric matrices, $\mathbf{z}\colon \Omega \to \mathbb{R}^n$, $\Omega \subset \mathbb{R}^2$, and $S\colon \mathbb{R}^n \to \mathbb{R}$. Despite much research, no well-defined high-order multisymplectic integrators are known for this class. We introduce a class of general purpose multisymplectic integrators for (1.1) that are locally well defined and can have high order in space and time.

Many variational PDEs and many nonlinear hyperbolic PDEs can be written in the form (1.1). For example, by introducing $\mathbf{z} = (u, v, w)$, $v = u_t$, and $w = u_x$, the wave equation $u_{tt} - u_{xx} = f(u)$ can be written in this form with

$$K = \begin{pmatrix} 0 & -1 & 0 \\ 1 & 0 & 0 \\ 0 & 0 & 0 \end{pmatrix}, \quad L = \begin{pmatrix} 0 & 0 & 1 \\ 0 & 0 & 0 \\ -1 & 0 & 0 \end{pmatrix}, \tag{1.2}$$

$$S(\mathbf{z}) = -V(u) + \frac{1}{2}v^2 - \frac{1}{2}w^2, \text{ and } f(u) = V'(u). \tag{1.3}$$

Any solutions to (1.1) satisfy the *multisymplectic conservation law*

$$\omega_t + \kappa_x = 0, \tag{1.4}$$

where $\omega = \frac{1}{2}(d\mathbf{z} \wedge Kd\mathbf{z})$ and $\kappa = \frac{1}{2}(d\mathbf{z} \wedge Ld\mathbf{z})$ [16, p. 338]. A numerical method that satisfies a discrete version of (1.4) is called a *multisymplectic integrator*; see [16, 4] for reviews of multisymplectic integration.

The (Preissman or Keller) box scheme [16, p. 342], a multisymplectic integrator, is simply the implicit midpoint rule (a Runge–Kutta method) applied in space and in time on a rectangular grid. We call it the *simple box scheme* to distinguish it from

*Submitted to the journal's Methods and Algorithms for Scientific Computing section February 24, 2014; accepted for publication (in revised form) October 29, 2014; published electronically February 10, 2015. This research was supported by the Marsden Fund of the Royal Society of New Zealand.
http://www.siam.org/journals/sisc/37-1/95835.html

†Institute of Fundamental Sciences, Massey University, Private Bag 11 222, Palmerston North 4442, New Zealand (r.mclachlan@massey.ac.nz, mrmattwilkins@gmail.com).

other Runge–Kutta box-based schemes. There are plenty of multisymplectic low-order methods applicable to Schrödinger's equation [6, 11, 12, 17, 27, 31]. Most are based on box-like schemes and are second-order. LingHua's [15] method for the Klein–Gordon–Schrödinger equation has spectral accuracy in space and is second-order in time. Jia-Xiang, Bin, and Hua [14] present a multisymplectic, low-order, implicit/explicit method for the Klein–Gordon–Schrödinger equation. Hong and Li [10] present a box-like multisymplectic method for the nonlinear Dirac equation. For the Korteweg–de Vries equation there are numerous [10, 29, 30, 1] multisymplectic low-order box-like schemes. Moore and Reich [21] give a multisymplectic box-like low-order scheme that can be applied to any multi-Hamiltonian system. Bridges and Reich [3] present a staggered-grid multisymplectic method that is based on the symplectic Störmer–Verlet scheme. They discuss possible extensions to higher-order methods.

Although multisymplecticity by itself does not ensure good performance on traditional criteria like accuracy and stability, multisymplectic methods do have a number of advantages. They are (essentially) variational, the variational principle being considered fundamental to this class of physical law. They are the standard discrete model in the relevant parts of physics, such as the lattice dynamics of solid state physics. Symplecticity in space is essential for a semidiscretization to be amenable to symplectic time integration, whose advantages in long-time integration are well known. At the opposite extreme, steady-state solutions of (1.1) obey a Hamiltonian ODE in space. Methods that are not symplectic in space will typically preserve only the very simplest steady-state solutions, such as constants; methods that are symplectic in space can also preserve periodic, quasi-periodic, and heteroclinic solutions [19]. Standard methods for simple equations, such as those in [7], are multisymplectic.[1] For further discussion, and numerical comparisons of multisymplectic with nonsymplectic integrators, see [2, 13].

However, multisymplectic integrators can only preserve some conservation laws, and these do not typically include those of energy and momentum, which can be important for nonlinear stability. The issue is discussed further in [5, 26]; a full understanding of the relations between discrete conservation laws and discrete multisymplecticity, and their numerical implications, is still lacking.

In this paper, instead of discretizing one particular PDE, we wish to develop methods that are applicable to the entire class (1.1), specializing to a particular equation or family as late as possible. The simple box scheme is simple to define, can in principle be applied to any PDE of the form (1.1), and has several appealing properties, including the unconditional preservation of dispersion relations (up to a diffeomorphic remapping of continuous to discrete frequencies) with consequent lack of parasitic waves [2] and preservation of the sign of group velocities [8], and lack of spurious reflections at points where the mesh size changes [9]. These properties are related to the linearity of the box scheme; we consider methods that retain this feature.[2]

[1] Cohen [7, p. 34] writes, "all the schemes described below will be centered, since uncentered schemes generate numerical dissipation for wave equations which satisfy a principle of energy conservation." For the linear PDEs he considers, centered symmetric schemes are multisymplectic.

[2] A method is *linear in z* if it is equivariant with respect to linear changes of the dependent variables, $z \mapsto \tilde{z} := Az$. Runge–Kutta methods and linear multistep methods are linear in this sense, while partitioned Runge–Kutta methods are not. For this concept to be make sense, the method has to be defined for all systems obtained by such changes of variables; it does not apply to methods that are defined for a *single* differential equation.

However, the simple box scheme also has some less positive features. It is fully implicit, which makes it expensive; for equations where the CFL condition is not too restrictive, the extra (linear and sometimes nonlinear) stability this provides is not needed. The implicit equations may not have a solution: with periodic boundary conditions, solvability requires that the number of grid points be odd [23]; we have found no general treatment of Dirichlet, Neumann, or mixed boundary conditions in the literature that leads to a well-posed method. It is only second-order in space and time.

The latter issue can be avoided by applying higher-order Runge–Kutta methods in space and in time [22]. As the dependent variables are the internal stages, typically one obtains the stage order in space, for example, order r for r-stage Gauss Runge–Kutta [20]. However, the scheme is still fully implicit and this time leads to singular ODEs for periodic boundary conditions unless r and N are *both* odd [23, 20].

The first two issues, implicitness and boundary treatment, are related. They can be avoided for some PDEs, like the nonlinear wave equation, by applying suitable partitioned Runge–Kutta methods [23, 18, 24, 25]. *When they apply*, they can be excellent methods, leading to explicit ODEs amenable to explicit time-stepping, arbitrary order, and local boundary handling [20]. For example, the 5-point stencil for $u_{tt} - u_{xx} = f(u)$, equivalent to leapfrog in space and time, is a method of this class (2-stage Lobatto IIIA–IIIB). This class coincides in some cases with staggered grid methods, which again rely on the detailed structure of the equation, and can be extremely effective. However, the partitioning/staggering means that they are not linear methods, which can lead to, for example, discontinuous dispersion relations [20].

For Hamiltonian ODEs there are methods that are symplectic and methods that are not; and symplectic methods that are implicit and explicit; methods that are linearly equivariant and methods that are not; and methods defined for all ODEs and methods defined only for particularly structured ODEs. All approaches have their domains of applicability. While there are truly fundamental differences between Hamiltonian PDEs and ODEs, this situation indicates that there may be multisymplectic integrators based on Runge–Kutta discretizations that respect the structure of the PDE better than those previously known that lead to broader applicability. This is the case, and we introduce in this paper the class of *diamond schemes* for (1.1). It is based on the following observation. Let the PDE (1.1) be discretized on a square cell by a Runge–Kutta method in space and time. To each internal point there are n equations and n unknowns. To each pair of opposite edge points there is one equation. Therefore, to get a closed system with the same number of equations as unknowns, data should be specified on exactly *half* the edge points. We shall show later that for the nonlinear wave equation, specifying z at the edge points on two adjacent edges leads to a properly determined system for the two opposite edges. What remains is to arrange the cells so that the information flow is consistent with the initial value problem.

Definition 1. *A* diamond scheme *for the PDE* (1.1) *is a quadrilateral mesh in space-time together with a mapping of each quadrilateral to a square upon which a set of Runge–Kutta methods are applied in each dimension. Initial data is specified at sufficient edge points such that the solution can be propagated forward in time by locally solving for pairs of adjacent edges.*

For equations that are symmetric in x, the quadrilaterals are typically diamonds, and we outline the scheme first in section 2 in the simplest case, the analogue of the simple box scheme that we call the *simple diamond scheme*. The validity of

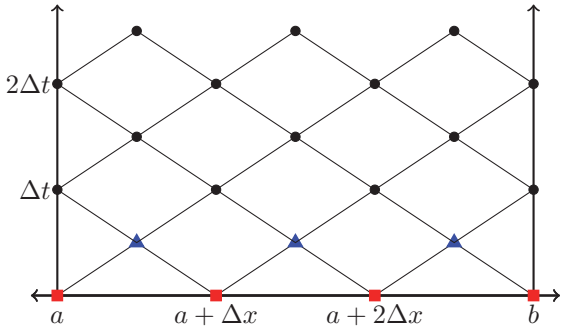

FIG. 1. *The domain divided into diamonds by the simple diamond method. The solution,* $\mathbf{z}$*, is calculated at the corners of the diamonds. The scheme is started using the initial condition, which gives the solution along the* x *axis at the red squares, and the solution at* $t = \frac{\Delta t}{2}$ *(the blue triangles), which is calculated using a forward Euler step. After this initialization the simple diamond scheme proceeds, step by step, to update the top of a diamond using the other three known points in that diamond.*

the method is illustrated on a nonlinear wave equation. We introduce the general diamond scheme, based on r-stage Gauss Runge–Kutta, in section 3. We prove that it is multisymplectic in general and that, for the nonlinear wave equation (1.2), it is well-defined, i.e., the algebraic equations have a solution for a sufficiently small time step. (The method does lead to a closed system of m equations in m unknowns for any multi-Hamiltonian PDE, but their solvability could depend on the PDE.) The validity of the method is illustrated on a nonlinear wave equation, and high convergence orders are observed; as the dependent variables are the *stage* variables of the underlying Runge–Kutta method, this order is related to the stage order, not the classical order, of the Runge–Kutta method. The dispersion relation, and hence the linear stability, of the simple diamond scheme is determined in section 4 for all multi-Hamiltonian PDEs. As the diamond scheme is implicit in z, but explicit in x, its obeys a CFL-type stability restriction typical of fully explicit methods. Section 5 concludes.

The diamond scheme is inspired by and has some similarities with the *staircase method* in discrete integrability [28]. In both cases initial data is posed on a subset of a quadrilateral graph such that the remaining data can be filled in uniquely. In discrete integrability, this fill-in is usually explicit, whereas for the diamond schemes it depends on the PDE and is usually implicit. A second key point is that in the diamond method, there is a stability condition that the fill-in must be such that the numerical domain of dependence includes the analytic domain of dependence. Thus the characteristics of the PDE determine the geometry of the mesh: if they all pointed to the right, then one could indeed use a simple rectangular mesh and fill in from left to right. (Indeed, this was how early versions of the box scheme proceeded.)

2. The simple diamond scheme. Consider solving (1.1) numerically on the domain $x \in [a, b]$, $t \geq 0$, with periodic boundary conditions. Unlike a typical finite difference scheme which uses a rectilinear grid aligned with the (x, t) axes, the simple diamond scheme uses a mesh comprising diamonds; see Figure 1.

To describe the simple diamond scheme consider a more detailed view of a single diamond in Figure 2: $\mathbf{z}_0^1$ is the solution at the top, $\mathbf{z}_1^0$ the rightmost point, $\mathbf{z}_0^{-1}$ the bottom, and $\mathbf{z}_{-1}^0$ the left. The point in the center of the diamond, $\mathbf{z}_0^0$, is defined as the average of the corner values.

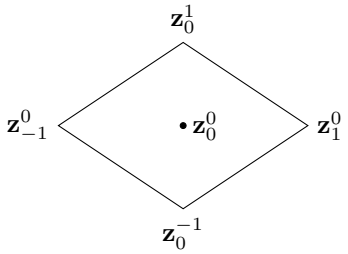

FIG. 2. *A single diamond in the simple diamond scheme. A diamond has a width of Δx and height of Δt.*

The discrete version of (1.1) is

$$K\left(\frac{\mathbf{z}_0^1-\mathbf{z}_0^{-1}}{\Delta t}\right)+L\left(\frac{\mathbf{z}_1^0-\mathbf{z}_{-1}^0}{\Delta x}\right)=\nabla S(\mathbf{z}_0^0), \tag{2.1}$$

$$\mathbf{z}_0^0=\frac{1}{4}\left(\mathbf{z}_0^1+\mathbf{z}_1^0+\mathbf{z}_0^{-1}+\mathbf{z}_{-1}^0\right). \tag{2.2}$$

The values $\mathbf{z}_1^0$, $\mathbf{z}_0^{-1}$, and $\mathbf{z}_{-1}^0$ are known from the preceding step, and $\mathbf{z}_0^0$ is determined from (2.2), leaving the n unknowns $\mathbf{z}_0^1$ to be determined from the n equations (2.1). The simple diamond scheme solves this system of equations independently for each diamond at each time step, then advances to the next step. To determine the local truncation error of this scheme, substitute the exact solution $\mathbf{z}(x+i\frac{\Delta x}{2},t+j\frac{\Delta t}{2})$ for $\mathbf{z}_i^j$ into (2.1) and expand in Taylor series:

$$K\left(\mathbf{z}_t+\frac{\Delta t^2}{4}\mathbf{z}_{ttt}+\mathcal{O}\left(\Delta t^3\right)\right)+L\left(\mathbf{z}_x+\frac{\Delta x^2}{4}\mathbf{z}_{xxx}+\mathcal{O}\left(\Delta x^3\right)\right)=\nabla S(\mathbf{z}) \tag{2.3}$$

$$\Rightarrow K\mathbf{z}_t+L\mathbf{z}_x=\nabla S(\mathbf{z})+\mathcal{O}\left(\Delta t^2+\Delta x^2\right); \tag{2.4}$$

thus the order is $\mathcal{O}\left(\Delta t^2+\Delta x^2\right)$.

For the one-dimensional wave equation defined by (1.1) and (1.2) the simple diamond scheme becomes

$$\frac{u_1^0-u_{-1}^0}{\Delta x}=\frac{w_0^{-1}+w_1^0+w_{-1}^0+w_0^1}{4}, \tag{2.5}$$

$$\frac{u_0^1-u_0^{-1}}{\Delta t}=\frac{v_0^{-1}+v_1^0+v_{-1}^0+v_0^1}{4}, \tag{2.6}$$

$$\frac{v_0^1-v_0^{-1}}{\Delta t}=\frac{w_1^0-w_{-1}^0}{\Delta x}+f(u_0^0). \tag{2.7}$$

At each time step, for each diamond, (2.5) is first solved to give the new w_0^1. Then (2.6) is solved for v_0^1 and substituted into (2.7) to give a scalar equation of the form

$$u_0^1=C+\frac{(\Delta t)^2}{4}f(u_0^0) \tag{2.8}$$

for u_0^1, where C depends on the known data. This equation has a solution $u_0^1=C+\mathcal{O}\left((\Delta t)^2\right)$ for sufficiently small Δt when f is Lipschitz. Thus, although the

scheme is implicit, it is only *locally* implicit within each cell; a set of N uncoupled scalar equations is typically much easier to solve than a system of N coupled equations.

PROPOSITION 2. *The simple diamond scheme shown in* (2.1) *satisfies the discrete conservation law*

$$\frac{1}{4\Delta t}\left((d\mathbf{z}^0_{-1}+d\mathbf{z}^1_0+d\mathbf{z}^0_1)\wedge Kd\mathbf{z}^1_0-(d\mathbf{z}^0_{-1}+d\mathbf{z}^{-1}_0+d\mathbf{z}^0_1)\wedge Kd\mathbf{z}^{-1}_0\right)$$
$$+\frac{1}{4\Delta x}\left((d\mathbf{z}^1_0+d\mathbf{z}^0_1+d\mathbf{z}^{-1}_0)\wedge Ld\mathbf{z}^0_1-(d\mathbf{z}^1_0+d\mathbf{z}^0_{-1}+d\mathbf{z}^{-1}_0)\wedge Ld\mathbf{z}^0_{-1}\right)=0.$$

Proof. Take the exterior derivative and apply $d\mathbf{z}^0_0\wedge$ on the left of (2.1) to give

$$\tfrac{1}{4\Delta t}(d\mathbf{z}^0_{-1}+d\mathbf{z}^1_0+d\mathbf{z}^0_1+d\mathbf{z}^{-1}_0)\wedge K(d\mathbf{z}^1_0-d\mathbf{z}^{-1}_0)$$
$$+\tfrac{1}{4\Delta x}(d\mathbf{z}^1_0+d\mathbf{z}^0_1+d\mathbf{z}^{-1}_0+d\mathbf{z}^0_{-1})\wedge L(d\mathbf{z}^0_1-d\mathbf{z}^0_{-1})=0.$$

Expanding and simplifying leads to the result. ∎

Numerical test. To illustrate the validity of the method, the Sine–Gordon equation, $u_{tt}-u_{xx}=-\sin(u)$ will be solved using the leapfrog and the simple diamond schemes. The leapfrog scheme used is

$$\frac{u_i^{j+1}-2u_i^j+u_i^{j-1}}{(\Delta t)^2}-\frac{u_{i-1}^j-2u_i^j+u_{i+1}^j}{(\Delta x)^2}=-\sin(u_i^j),$$

where Δt and Δx are the same as in the diamond grid, so the five-point stencil contains four diamonds. An exact solution is the so-called breather,

$$u(x,t)=4\arctan\left(\frac{\sin\left(\frac{t}{\sqrt{2}}\right)}{\cosh\left(\frac{x}{\sqrt{2}}\right)}\right). \tag{2.9}$$

The domain is taken significantly large, $[-30,30]$, so the solution can be assumed periodic. The initial conditions are calculated using the exact solution. The error is the discrete 2-norm of u,

$$E^2=\frac{b-a}{N}\sum_i^N\left(\tilde{u}_i-u(a+i\Delta x,T)\right)^2. \tag{2.10}$$

Figure 3 shows the error of both schemes as Δt is reduced while keeping the Courant number $\frac{\Delta t}{\Delta x}=\frac{1}{2}$. The integration time $T=1.5$ is twice the largest time step. It is apparent that for this problem, both schemes appear to have order 2.

Boundary conditions. Because the simple diamond scheme is locally defined, boundary conditions can be treated locally without affecting the solvability of the discrete equations. The numerical method requires n conditions at each boundary, and the PDE typically provides fewer than n. Extra conditions can be found by (i) differentiating the boundary conditions in the direction of the boundary; (ii) using and/or differentiating the PDE at the boundary; and (iii) utilizing a phantom diamond that straddles the boundary. We illustrate here one possible treatment of Dirichlet and Neumann boundary conditions. For the nonlinear wave equation with Dirichlet condition $u(a,t)=f(t)$, the values of $u(a,n\Delta t)=f(n\Delta t)$ are given, and by

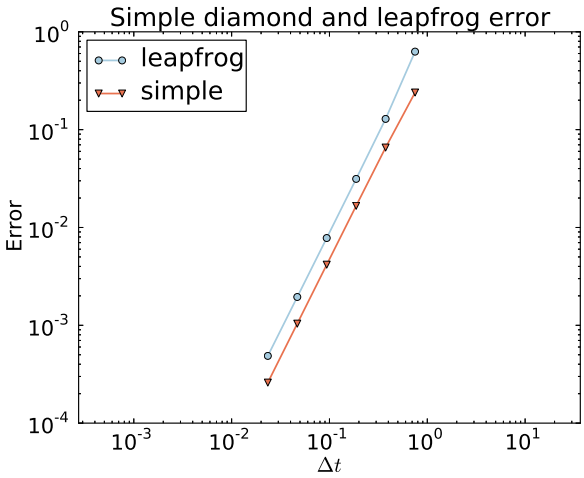

FIG. 3. *The error of the simple diamond scheme applied to the multisymplectic Hamiltonian PDE arising from the Sine–Gordon equation, and the error of the leapfrog scheme applied to the Sine-Gordon equation. The exact solution is the so-called breather on the domain* $[-30, 30]$. *The Courant number is fixed at* $\frac{1}{2}$ *as* Δt *is decreased. Both methods appear to have order* 2.

differentiating the boundary condition, $v(a, n\Delta t) = f'(n\Delta t)$ can be found. From the PDE we have $w_t = v_x$, and using the approximation

$$A = v_x\left(a, \left(n - \tfrac{1}{2}\right)\Delta t\right) \approx \frac{v(a + \frac{1}{2}\Delta x, (n - \frac{1}{2})\Delta t) - f'((n - \frac{1}{2})\Delta t)}{\frac{1}{2}\Delta x},$$

gives the update $w(a, n\Delta t) = w(a, (n-1)\Delta t) + \Delta t A$. For the Neumann condition $u_x(b, t) = g(t)$, a phantom diamond is used. First fill in the values of $\mathbf{z}_1^0$ (see Figure 2): the boundary condition provides w_0^0, and linear extrapolation provides w_1^0; the boundary condition provides u_x at the center point, and linear extrapolation from u_{-1}^0 provides u_1^0; the PDE implies $v_x = w_t$, where w_t is provided by the boundary condition at the center point, and linear extrapolation from v_{-1}^0 provides v_1^0. The boundary diamond is then filled in like the internal diamonds. Figure 4 shows the results of 150,000 steps of the simple diamond scheme together with this boundary treatment, for the linear wave equation for a solution that contains both left- and right-moving waves.

3. The diamond scheme. The diamond scheme refines the simple diamond scheme discretization by using the multisymplectic Runge–Kutta collocation method given by Reich [22] within each diamond. It is easier to apply this method to a square that is aligned with the axes, so the first step is to transform the (x, t) coordinate space. Each diamond in Figure 1 is transformed to a square of side length one using the linear transformation T defined by

$$T: \quad \tilde{x} = \tfrac{1}{\Delta x}x + \tfrac{1}{\Delta t}t \quad \text{and} \quad \tilde{t} = -\tfrac{1}{\Delta x}x + \tfrac{1}{\Delta t}t. \tag{3.1}$$

Because (1.1) has no dependence on x or t it doesn't matter where the square is located in $(\tilde{x}, \tilde{t})$ space, so the same transformation can be used for all the diamonds. Let $\tilde{\mathbf{z}}(\tilde{x}, \tilde{t}) = \mathbf{z}(x, t)$. By the chain rule

$$\mathbf{z}_x = \tilde{\mathbf{z}}_{\tilde{x}}\tfrac{1}{\Delta x} - \tilde{\mathbf{z}}_{\tilde{t}}\tfrac{1}{\Delta x} \quad \text{and} \quad \mathbf{z}_t = \tilde{\mathbf{z}}_{\tilde{x}}\tfrac{1}{\Delta t} + \tilde{\mathbf{z}}_{\tilde{t}}\tfrac{1}{\Delta t}, \tag{3.2}$$

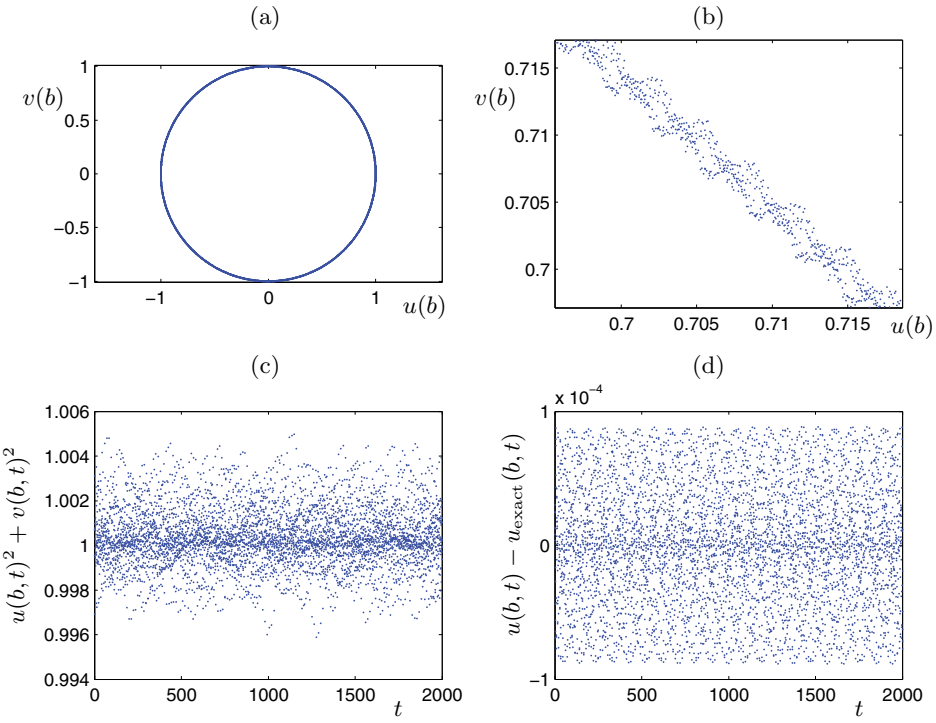

FIG. 4. *Solution of the linear wave equation on* $[a,b]$ *with Dirichlet boundary condition* $u(a,t) = \sin a \cos t$*, Neumann boundary condition* $u_x(b,t) = -\cos a \cos t$*,* $a = 0.5$*,* $b = \pi/2$*, and exact solution* $u(x,t) = \sin x \cos t$ *which contains both left- and right-moving waves. There are* $N = 40$ *diamonds in space and the Courant number is* 0.5*;* 150,000 *time steps are shown. See text for the handling of the boundary conditions.* (a) *Phase portrait of* $(u(b,t), v(b,t))$*, which is a circle in the exact solution.* (b) *Close-up of* (a) *showing some blurring of the orbit, which does not increase in time.* (c) *Evolution of local energy* $u(b,t)^2 + v(b,t)^2$ *at* $x = b$ *versus time (exact value is* 1*); the error does not increase in time.* (d) *Global error in* $u(b,t)$ *versus. time. The error does not increase in time. (Note that* $u(b,t)$ *is not fixed by the boundary condition.)*

so

$$\begin{aligned} K\mathbf{z}_t + L\mathbf{z}_x &= K\left(\tilde{\mathbf{z}}_{\tilde{x}}\tfrac{1}{\Delta t} + \tilde{\mathbf{z}}_{\tilde{t}}\tfrac{1}{\Delta t}\right) + L\left(\tilde{\mathbf{z}}_{\tilde{x}}\tfrac{1}{\Delta x} - \tilde{\mathbf{z}}_{\tilde{t}}\tfrac{1}{\Delta x}\right) \\ &= \left(\tfrac{1}{\Delta t}K - \tfrac{1}{\Delta x}L\right)\tilde{\mathbf{z}}_{\tilde{t}} + \left(\tfrac{1}{\Delta t}K + \tfrac{1}{\Delta x}L\right)\tilde{\mathbf{z}}_{\tilde{x}}, \end{aligned}$$

and thus (1.1) transforms to

$$\tilde{K}\tilde{\mathbf{z}}_{\tilde{t}} + \tilde{L}\tilde{\mathbf{z}}_{\tilde{x}} = \nabla S(\tilde{\mathbf{z}}), \tag{3.3}$$

where

$$\tilde{K} = \tfrac{1}{\Delta t}K - \tfrac{1}{\Delta x}L \quad \text{and} \quad \tilde{L} = \tfrac{1}{\Delta t}K + \tfrac{1}{\Delta x}L. \tag{3.4}$$

Outline of method. Figure 5 illustrates the diamond scheme for a sample initial-boundary value problem on $[a,b] \times \mathbb{R}^+$ with periodic boundary conditions. The solution $\mathbf{z}$ is calculated at grid points located on the solid diamond edges; dashed edges indicate where values are inferred by periodicity. Information follows from the bottom left and right edges of a diamond to the top left and right edges of the same

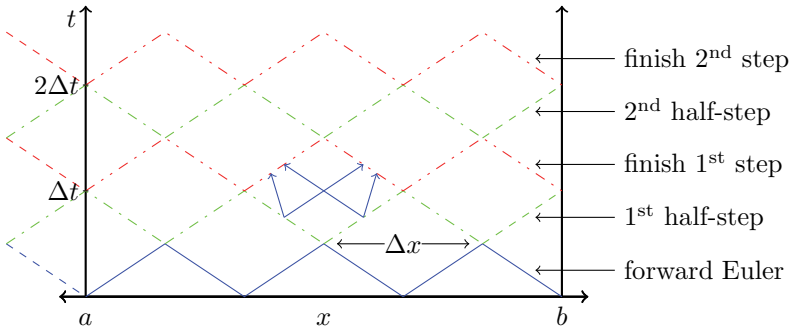

FIG. 5. *Information flows upward as indicated by the solid blue arrows for a typical diamond. The solution,* $\mathbf{z}$*, is initialized on the solid blue zig-zag line. A step of the diamond scheme consists of two half-steps. The first half-step calculates* $\mathbf{z}$ *along the green dash-dot line, which by periodicity is extended to the dashed line to the right. The second half-step uses the green dash-dot line to calculate the red dash-double-dotted line, which again by periodicity is extended to the left-hand dashed segment.*

diamond. An initialization step must provide values for $\mathbf{z}$ along the bottom edges of the first row of diamonds (the first solid blue zig-zag line in the figure). This is extended using periodicity beyond the left-hand boundary (the blue dashed line). The initialization should not reduce the overall order nor undo special numerical properties of the scheme. In this paper the known exact solution has been used; however, an initialization method of high order has been developed and will be presented in future work. A step of the diamond scheme consists of two half-steps. The first half-step calculates $\mathbf{z}$ along the top edges of the first row of diamonds (green dash-dot zig-zag), which by periodicity is extended to the right-hand boundary (the green dashed line). The second half-step uses values on the top edges of the first row of diamonds (green dash-dot line) to calculate the new values of $\mathbf{z}$ on the top edges of the second row (red dash-double-dotted line). Again by periodicity the values from the top right edge of the rightmost diamond are copied outside the left-hand boundary of the domain (the red dashed segment). Another step can be performed now using the red dash-double-dotted zig-zag as initial data (the very-right-hand line segment is not used except to provide values for the dashed line).

Updating one diamond. Let (A, b, c) be the parameters of an r-stage Runge–Kutta method. In what follows, we will take the method to be the Gauss Runge–Kutta method. Figure 6 shows a diamond with $r = 3$ and its transformation to the unit square. The square contains $r \times r$ internal grid points, as determined by the Runge–Kutta coefficients c, and internal stages $\mathbf{Z}_i^j$, which are analogous to the usual internal grid points and stages in a Runge–Kutta method. The internal stages also carry the variables $\mathbf{X}_i^j$ and $\mathbf{T}_i^j$ which approximate z_x and z_t, respectively, at the internal stages.

The dependent variables of the method are the values of z at the edge grid points. To be able to distinguish the internal edge points from all the edge points let I be the set of indices $\{1, \ldots, r\}$. Then, for example, $\tilde{\mathbf{z}}_I^{\mathrm{b}}$ refers to $\tilde{\mathbf{z}}_i^{\mathrm{b}}, i = 1, \ldots, r$. If the I qualifier does not appear, then the left- or bottommost corner is included, for example, $\tilde{\mathbf{z}}^{\mathrm{b}}$ refers to the points $\tilde{\mathbf{z}}_i^{\mathrm{b}}, i = 0, \ldots, r$, but does not include $\tilde{\mathbf{z}}_{r+1}^{\mathrm{b}}$ which is $\tilde{\mathbf{z}}_{\mathrm{r}}^0$. Note $\tilde{\mathbf{z}}_0^{\mathrm{b}} = \tilde{\mathbf{z}}_\ell^0$ (which is also the same as $\mathbf{z}_0^{-1}$). The Runge–Kutta discretization is

$$\mathbf{Z}_i^j = \tilde{\mathbf{z}}_\ell^j + \sum_{k=1}^{r} a_{ik} \mathbf{X}_k^j, \tag{3.5}$$

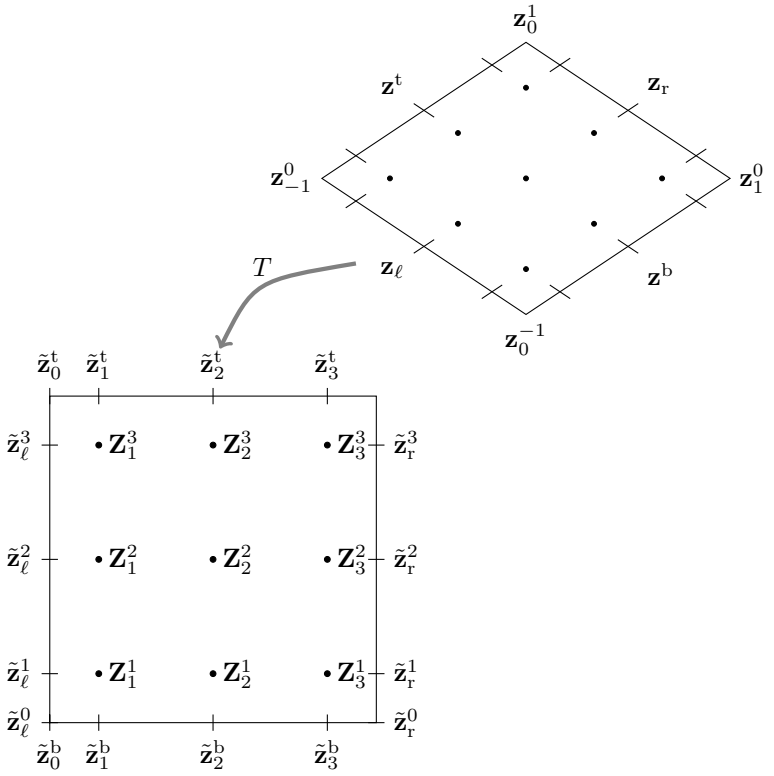

FIG. 6. *The diamond transformed by a linear transformation, T, to the unit square. The square contains $r \times r$ ($r = 3$ in this example) internal stages, $\mathbf{Z}_i^j$. The solution is known along the bottom and left-hand sides. The method proceeds as two sets of r Gauss Runge–Kutta r-step methods: internal stage values, $\mathbf{Z}_i^j$, $\mathbf{X}_i^j$, $\mathbf{T}_i^j$, are calculated, then the right and top are updated.*

$$\mathbf{Z}_i^j = \tilde{\mathbf{z}}_i^{\mathrm{b}} + \sum_{k=1}^{r} a_{jk} \mathbf{T}_i^k, \tag{3.6}$$

$$\nabla S(\mathbf{Z}_i^j) = \tilde{K} \mathbf{T}_i^j + \tilde{L} \mathbf{X}_i^j, \tag{3.7}$$

together with the update equations

$$\tilde{\mathbf{z}}_{\mathrm{r}}^i = \tilde{\mathbf{z}}_\ell^i + \sum_{k=1}^{r} b_k \mathbf{X}_k^i, \tag{3.8}$$

$$\tilde{\mathbf{z}}_i^{\mathrm{t}} = \tilde{\mathbf{z}}_i^{\mathrm{b}} + \sum_{k=1}^{r} b_k \mathbf{T}_i^k, \tag{3.9}$$

for $i, j \in I$. The $\tilde{\mathbf{z}}_\ell^I$ and $\tilde{\mathbf{z}}_I^{\mathrm{b}}$ are known. Equations (3.5)–(3.7) are first solved for the internal stage values $\mathbf{Z}_i^j$, $\mathbf{X}_i^j$, and $\mathbf{T}_i^j$, then (3.8) and (3.9) are used to calculate $\tilde{\mathbf{z}}_I^{\mathrm{t}}$ and $\tilde{\mathbf{z}}_{\mathrm{r}}^I$. Equations (3.5)–(3.7) are $3r^2$ equations in $3r^2$ unknowns $\mathbf{Z}$, $\mathbf{X}$, and $\mathbf{T}$. Equations (3.5) and (3.6) are linear in $\mathbf{X}$ and $\mathbf{T}$. Thus in practice the method requires solving a set of $r^2 n$ nonlinear equations for $\mathbf{Z}$ in each diamond.

The method does not use values at the corners. However, if solutions are wanted at the corners, then the method can be extended by allowing $j = 0$ in (3.5) and associating $\mathbf{Z}_i^0$ with $\tilde{\mathbf{z}}_i^{\mathrm{b}}$ and allowing $i = 0$ in (3.6) and associating $\mathbf{Z}_0^j$ with $\tilde{\mathbf{z}}_\ell^j$. This

extension gives equations for $\mathbf{X}_k^0$ and $\mathbf{T}_0^k$, which can be used in the update equations (3.8) and (3.9) which are extended by allowing $i = 0$. On this extended domain (3.5)–(3.7) are $2r(r+1) + r^2$ equations. This is because (3.5) is extended onto the bottom boundary ($r(r+1)$ equations) and (3.6) onto the left boundary ($r(r+1)$ equations), but there is no need to extend (3.7) onto either boundaries because $\mathbf{T}$ was not extended onto the bottom boundary, and $\mathbf{X}$ was not extended onto the left boundary. The number of unknowns is $2r(r+1) + r^2$, so again there is the same number of equations as unknowns. Corner points are shared by two adjacent diamonds, and typically $\tilde{\mathbf{z}}_{r+1}^{\mathrm{b}} \neq \tilde{\mathbf{z}}_{\ell}^{r+1}$. In practice the mean of these two approximations is used.

Here is a summary of the diamond scheme algorithm:

Let $\mathbf{z}$ and $\mathbf{z}_n$ be $N(2r+1)$ length vectors with each element in $\mathbb{R}^n$. These vectors contain the $\tilde{\mathbf{z}}$ values for two particular edges of each diamond. Each of the two edges has r nodes, plus there is the value at the bottom, hence $2r+1$ values per N diamonds.

1. Initialize $\mathbf{z}$. It now contains $\tilde{\mathbf{z}}$ for the blue zig-zag at the bottom in Figure 5.
2. The half-step. For each diamond;
   (a) associate $\tilde{\mathbf{z}}_\ell$ and $\tilde{\mathbf{z}}^{\mathrm{b}}$ with the correct values in $\mathbf{z}$ (periodicity is used at the edges);
   (b) solve (3.5)–(3.7);
   (c) use (3.8) and (3.9) to find $\tilde{\mathbf{z}}_{\mathrm{r}}$ and $\tilde{\mathbf{z}}^{\mathrm{t}}$;
   (d) associate $\tilde{\mathbf{z}}_{\mathrm{r}}$ and $\tilde{\mathbf{z}}^{\mathrm{t}}$ with the current diamond's section of $\mathbf{z}_n$ (periodicity is used at the edges).
3. $\mathbf{z} = \mathbf{z}_n$. Now $\mathbf{z}$ contains $\tilde{\mathbf{z}}$ values for the second/green zig-zag in Figure 5.
4. Perform step 2 again.
5. $\mathbf{z} = \mathbf{z}_n$. Now $\mathbf{z}$ contains $\tilde{\mathbf{z}}$ values for the third/red zig-zag in Figure 5.
6. If final time not reached go to step 2.

THEOREM 3. *For the multi-Hamiltonian one-dimensional wave equation defined by* (1.1) *and* (1.2) *with the conditions*

- *f is Lipschitz with constant L;*
- *the matrix A of coefficients of the underlying Runge–Kutta scheme is invertible;*
- *the matrix*

$$B = (1-\lambda^2)(I \otimes A^{-2}) + 2(1+\lambda^2)(A^{-1} \otimes A^{-1}) + (1-\lambda^2)(A^{-2} \otimes I),$$

  is invertible, where $\lambda = \frac{\Delta t}{\Delta x}$ is the Courant number; and
- $\Delta t < 1/(L\|B^{-1}\|_\infty)^{1/2}$,

(3.5)–(3.7) *are solvable, and thus the diamond scheme is well defined.*

Proof. Equations. (3.5) and (3.6) relate components of matrices and tensors. Writing these equations in tensor form, then multiplying on the left by A^{-1}, gives expressions for $\mathbf{X}_i^j$ and $\mathbf{T}_i^j$. Substituting these into (3.7) gives

$$\nabla S(\mathbf{Z}_i^j) = \tilde{K} \sum_{k=1}^{r} m_{jk}(\mathbf{Z}_i^k - \mathbf{z}_i^{\mathrm{b}}) + \tilde{L} \sum_{k=1}^{r} m_{ik}(\mathbf{Z}_k^j - \mathbf{z}_\ell^k),$$

where m_{ij} are the elements of A^{-1}, and the tildes on the $\mathbf{z}$ values have been dropped for clarity. Using (3.4) for $\tilde{K}$ and $\tilde{L}$, and adopting the summation convention, this

becomes

$$\begin{pmatrix} -f(u_i^j) \\ v_i^j \\ -w_i^j \end{pmatrix} = \begin{pmatrix} 0 & \frac{-1}{\Delta t} & \frac{-1}{\Delta x} \\ \frac{1}{\Delta t} & 0 & 0 \\ \frac{1}{\Delta x} & 0 & 0 \end{pmatrix} m_{jk}(\mathbf{Z}_i^k - \mathbf{z}_i^{\mathrm{b}}) + \begin{pmatrix} 0 & \frac{-1}{\Delta t} & \frac{1}{\Delta x} \\ \frac{1}{\Delta t} & 0 & 0 \\ \frac{-1}{\Delta x} & 0 & 0 \end{pmatrix} m_{ik}(\mathbf{Z}_k^j - \mathbf{z}_\ell^k).$$

The solution for v_i^j and w_i^j,

$$\begin{aligned} v_i^j &= \frac{1}{\Delta t} m_{jk}(u_i^k - u_i^{\mathrm{b}}) + \frac{1}{\Delta t} m_{ik}(u_k^j - u_\ell^k), \\ w_i^j &= \frac{-1}{\Delta x} m_{jk}(u_i^k - u_i^{\mathrm{b}}) + \frac{1}{\Delta x} m_{ik}(u_k^j - u_\ell^k), \end{aligned}$$

is substituted into the equation for u_i^j, which after simplification gives

$$(1-\lambda^2) m_{jk} m_{kp} u_i^p + 2(1+\lambda^2) m_{jk} m_{ip} u_p^k + (1-\lambda^2) m_{ik} m_{kp} u_p^j = \mathbf{b} + (\Delta t)^2 f(u_i^j),$$

where the vector $\mathbf{b}$ is a constant term depending on A^{-1} and the initial data $\mathbf{z}_\ell$ and $\mathbf{z}^{\mathrm{b}}$. Let $\mathbf{u} = (u_1^1, u_1^2, \ldots, u_1^r, u_2^1, \ldots, u_3^1, \ldots, u_r^r)$ and $f(\mathbf{u}) = (f(u_1^1), \ldots, f(u_r^r))$; then this simplifies to

$$B\mathbf{u} = \mathbf{b} + \Delta t^2 f(\mathbf{u}), \tag{3.10}$$

where B is given in the conditions of the theorem. To complete the proof it must be shown that this equation has a solution. Because B is invertible, $G(\mathbf{u}) = B^{-1}(\mathbf{b} + \Delta t^2 f(\mathbf{u}))$ exists. Consider G applied to the two points $\mathbf{u}^1$ and $\mathbf{u}^2$,

$$\begin{aligned} \|G(\mathbf{u}^1) - G(\mathbf{u}^2)\|_\infty &= \Delta t^2 \|B^{-1}(f(\mathbf{u}^1) - f(\mathbf{u}^2))\|_\infty \\ &\le \Delta t^2 \|B^{-1}\|_\infty L \|\mathbf{u}^1 - \mathbf{u}^2\|_\infty. \end{aligned}$$

By the contraction mapping theorem and the condition on Δt, G must have a fixed point $\mathbf{u} = G(\mathbf{u})$, and thus (3.10) has a solution. ∎

For a particular Runge–Kutta method it is straightforward to calculate the matrix B and determine the conditions on λ that lead to solvability. Figure 7 shows that for Gauss Runge–Kutta, $r = 1, \ldots, 5$ and $\lambda \in [0, 1]$, the minimum singular value of B is nonzero. This calculation can be performed for larger r.

THEOREM 4. *The diamond scheme satisfies the discrete symplectic conservation law*

$$\frac{1}{\Delta t} \sum_{i=1}^{r} b_i(\omega_i^{\mathrm{t}} + \omega_{\mathrm{r}}^i - (\omega_\ell^i + \omega_i^{\mathrm{b}})) + \frac{1}{\Delta x} \sum_{i=1}^{r} b_i(\kappa_{\mathrm{r}}^i + \kappa_i^{\mathrm{b}} - (\kappa_i^{\mathrm{t}} + \kappa_\ell^i)) = 0,$$

where $\omega_n^m = \frac{1}{2} d\mathbf{z}_n^m \wedge K d\mathbf{z}_n^m$, $\kappa_n^m = \frac{1}{2} d\mathbf{z}_n^m \wedge L d\mathbf{z}_n^m$, *and* $m, n \in [0, r] \cup \{\mathrm{t}, \mathrm{r}, \mathrm{b}, \ell\}$ *(refer to Figure 6 for the definition of those labels).*

Proof. The solver within each square satisfies the discrete multisymplectic conservation law [23]

$$\Delta x \sum_{i=1}^{r} b_i(\tilde{\omega}_i^{\mathrm{t}} - \tilde{\omega}_i^{\mathrm{b}}) + \Delta t \sum_{i=1}^{r} b_i(\tilde{\kappa}_{\mathrm{r}}^i - \tilde{\kappa}_\ell^i) = 0,$$

where $\Delta x = \Delta t = 1$ because the square has side length one. Substituting in $\tilde{\omega}_n^m = \frac{1}{2} d\tilde{\mathbf{z}}_n^m \wedge \tilde{K} d\tilde{\mathbf{z}}_n^m$ and $\tilde{\kappa}_n^m = \frac{1}{2} d\tilde{\mathbf{z}}_n^m \wedge \tilde{L} d\tilde{\mathbf{z}}_n^m$ gives

$$\frac{1}{2} \sum_{i=1}^{r} b_i(d\tilde{\mathbf{z}}_i^{\mathrm{t}} \wedge \tilde{K} d\tilde{\mathbf{z}}_i^{\mathrm{t}} - d\tilde{\mathbf{z}}_i^{\mathrm{b}} \wedge \tilde{K} d\tilde{\mathbf{z}}_i^{\mathrm{b}} + d\tilde{\mathbf{z}}_{\mathrm{r}}^i \wedge \tilde{L} d\tilde{\mathbf{z}}_{\mathrm{r}}^i - d\tilde{\mathbf{z}}_\ell^i \wedge \tilde{L} d\tilde{\mathbf{z}}_\ell^i) = 0.$$

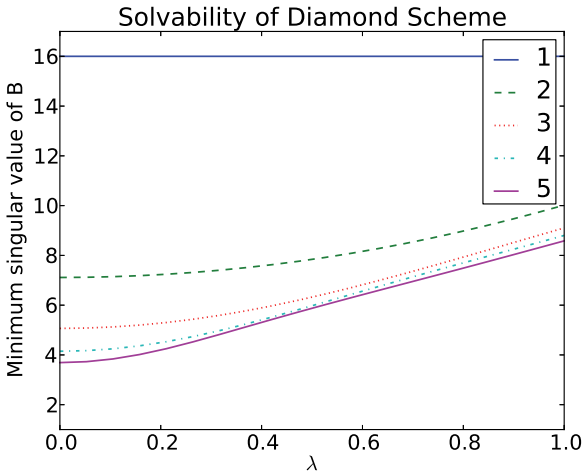

FIG. 7. *How the minimum singular value of B varies with different Courant numbers. Because there are no zero singular values, the diamond scheme is solvable for the wave equation for all $\lambda \in [0,1]$ and r up to 5. It is easy to check this holds for larger r.*

Using $d\tilde{\mathbf{z}}_n^m = d\mathbf{z}_n^m$, and (3.4) this becomes

$$\begin{aligned}
&\frac{1}{2}\sum_{i=1}^{r} b_i(d\mathbf{z}_i^{\mathrm{t}} \wedge (\tfrac{1}{\Delta t}K - \tfrac{1}{\Delta x}L)d\mathbf{z}_i^{\mathrm{t}} - d\mathbf{z}_i^{\mathrm{b}} \wedge (\tfrac{1}{\Delta t}K - \tfrac{1}{\Delta x}L)d\mathbf{z}_i^{\mathrm{b}} \\
&\qquad + d\mathbf{z}_{\mathrm{r}}^i \wedge (\tfrac{1}{\Delta t}K + \tfrac{1}{\Delta x}L)d\mathbf{z}_{\mathrm{r}}^i - d\mathbf{z}_\ell^i \wedge (\tfrac{1}{\Delta t}K + \tfrac{1}{\Delta x}L)d\mathbf{z}_\ell^i) = 0 \\
&\Rightarrow \frac{1}{\Delta t}\sum_{i=1}^{r} b_i(\omega_i^{\mathrm{t}} - \omega_i^{\mathrm{b}} + \omega_{\mathrm{r}}^i - \omega_\ell^i) + \frac{1}{\Delta x}\sum_{i=1}^{r} b_i(-\kappa_i^{\mathrm{t}} + \kappa_i^{\mathrm{b}} + \kappa_{\mathrm{r}}^i - \kappa_\ell^i) = 0. \qquad \square
\end{aligned}$$

We now examine the relationship between the simple diamond scheme (which uses corner values only) and the $r = 1$ diamond scheme (which uses edge values only). To relate the two, note that the extension to the corners of the $r = 1$ diamond scheme discussed previously, in which (3.5), (3.6), (3.8), (3.9) are applied with $i = j = 0$, leads on a single diamond to

$$\begin{aligned}
\tilde{\mathbf{z}}^{\mathrm{b}} &= \frac{\mathbf{z}_0^{-1} + \mathbf{z}_1^0}{2}, \quad \tilde{\mathbf{z}}^{\mathrm{t}} = \frac{\mathbf{z}_{-1}^0 + \mathbf{z}_0^1}{2}, \\
\tilde{\mathbf{z}}_\ell &= \frac{\mathbf{z}_0^{-1} + \mathbf{z}_{-1}^0}{2}, \quad \tilde{\mathbf{z}}_{\mathrm{r}} = \frac{\mathbf{z}_1^0 + \mathbf{z}_0^1}{2},
\end{aligned} \tag{3.11}$$

where the sub/superscript 1 has been dropped.

THEOREM 5. (i) *Any solution of the simple diamond scheme, mapped to edge midpoint values according to* (3.11)*, satisfies the equations of the $r = 1$ diamond scheme.* (ii) *Any solution of the $r = 1$ diamond scheme corresponds under* (3.11) *locally to a 1-parameter family of solutions to the simple diamond scheme. With periodic boundary conditions, the correspondence is global iff the solution satisfies $\sum_i \mathbf{z}_{\ell i,j}^1 = \sum_i \mathbf{z}_{1i,j}^{\mathrm{b}}$ for all j, where the subscript $_{i,j}$ refers to the ith diamond at the jth time step.*

Proof. When $r = 1$, (3.5)–(3.9) become

$$\mathbf{Z} = \tilde{\mathbf{z}}_\ell + \frac{1}{2}\mathbf{X}, \tag{3.12}$$

$$\mathbf{Z} = \tilde{\mathbf{z}}^{\mathrm{b}} + \frac{1}{2}\mathbf{T}, \tag{3.13}$$

$$\nabla S(\mathbf{Z}_1^1) = \tilde{K}\mathbf{T} + \tilde{L}\mathbf{X}, \tag{3.14}$$

$$\tilde{\mathbf{z}}_{\mathrm{r}} = \tilde{\mathbf{z}}_\ell + \mathbf{X}, \tag{3.15}$$

$$\tilde{\mathbf{z}}^{\mathrm{t}} = \tilde{\mathbf{z}}^{\mathrm{b}} + \mathbf{T}, \tag{3.16}$$

where $\tilde{K}$ and $\tilde{L}$ are the transformed K and L given in (3.4), and the sub/superscript 1 has been omitted in $\tilde{\mathbf{z}}_\ell$, $\tilde{\mathbf{z}}^{\mathrm{b}}$, $\tilde{\mathbf{z}}_{\mathrm{r}}$, $\tilde{\mathbf{z}}^{\mathrm{t}}$, $\mathbf{Z}$, $\mathbf{X}$, and $\mathbf{T}$.

Eliminating $\mathbf{X}$, $\mathbf{T}$, and $\mathbf{Z}$ from the five equations (3.12)–(3.16) yields the equivalent formulation

$$\tilde{K}\left(\tilde{\mathbf{z}}^{\mathrm{t}} - \tilde{\mathbf{z}}^{\mathrm{b}}\right) + \tilde{L}\left(\tilde{\mathbf{z}}_{\mathrm{r}} - \tilde{\mathbf{z}}_\ell\right) = \nabla S\left(\frac{\tilde{\mathbf{z}}^{\mathrm{t}} + \tilde{\mathbf{z}}^{\mathrm{b}} + \tilde{\mathbf{z}}_{\mathrm{r}} + \tilde{\mathbf{z}}_\ell}{4}\right), \tag{3.17}$$

$$\tilde{\mathbf{z}}^{\mathrm{t}} - \tilde{\mathbf{z}}_{\mathrm{r}} + \tilde{\mathbf{z}}^{\mathrm{b}} - \tilde{\mathbf{z}}_\ell = 0. \tag{3.18}$$

(i) Substituting the relations (3.11) into the equations of the simple diamond scheme (2.1) and (2.2) gives

$$\begin{aligned}
\nabla S\left(\frac{\mathbf{z}_0^{-1} + \mathbf{z}_{-1}^0 + \mathbf{z}_1^0 + \mathbf{z}_0^1}{4}\right) &= K\left(\frac{\mathbf{z}_0^1 - \mathbf{z}_0^{-1}}{\Delta t}\right) + L\left(\frac{\mathbf{z}_1^0 - \mathbf{z}_{-1}^0}{\Delta x}\right) \\
\Rightarrow \nabla S\left(\frac{\tilde{\mathbf{z}}^{\mathrm{t}} + \tilde{\mathbf{z}}^{\mathrm{b}} + \tilde{\mathbf{z}}_{\mathrm{r}} + \tilde{\mathbf{z}}_\ell}{4}\right) &= \tfrac{1}{\Delta t}K\left(\tilde{\mathbf{z}}^{\mathrm{t}} - \tilde{\mathbf{z}}^{\mathrm{b}} + \tilde{\mathbf{z}}_{\mathrm{r}} - \tilde{\mathbf{z}}_\ell\right) + \tfrac{1}{\Delta x}L\left(\tilde{\mathbf{z}}_{\mathrm{r}} - \tilde{\mathbf{z}}_\ell - \tilde{\mathbf{z}}^{\mathrm{t}} + \tilde{\mathbf{z}}^{\mathrm{b}}\right) \\
&= \left(\tfrac{1}{\Delta t}K - \tfrac{1}{\Delta x}L\right)\left(\tilde{\mathbf{z}}^{\mathrm{t}} - \tilde{\mathbf{z}}^{\mathrm{b}}\right) + \left(\tfrac{1}{\Delta t}K + \tfrac{1}{\Delta x}L\right)\left(\tilde{\mathbf{z}}_{\mathrm{r}} - \tilde{\mathbf{z}}_\ell\right) \\
&= \tilde{K}\left(\tilde{\mathbf{z}}^{\mathrm{t}} - \tilde{\mathbf{z}}^{\mathrm{b}}\right) + \tilde{L}\left(\tilde{\mathbf{z}}_{\mathrm{r}} - \tilde{\mathbf{z}}_\ell\right)
\end{aligned}$$

using (3.4), that is, the equations (3.17) of the $r = 1$ diamond scheme are satisfied. Equation (3.18) follows directly from (3.11).

(ii) Using (3.11), the corner values of one diamond can be recovered uniquely from the edge values and one corner value. From these values, adjacent diamonds can be filled in, continuing to get a unique solution for the corner values in any simply connected region. The same calculation as in part (i) now shows that these corner values satisfy the equations of the simple diamond scheme. For a global solution with periodic boundary conditions, the edge values at one time level j must lie in the range of the mean value operator in (3.11), which gives the condition in the theorem. (If the condition holds at $j = 1$, it holds for all j, from (3.18).) In both cases one corner value parameterizes the solutions. ∎

Theorem 5 implies that under (3.11), the multisymplectic conservation laws of the simple and $r = 1$ diamond schemes are equivalent. This is now proved directly.

COROLLARY 6. *Under the relations* (3.11)*, the simple diamond scheme and the* $r = 1$ *diamond scheme have equivalent discrete multisymplectic conservation laws.*

Proof. Substitute $r = 1$ into Theorem 4, note $b_1 = 1$, and differentiate (3.11) to get $d\mathbf{z}_1^{\mathrm{t}} = (d\mathbf{z}_0^1 + d\mathbf{z}_{-1}^0)/2$, $d\mathbf{z}_{\mathrm{r}}^1 = (d\mathbf{z}_0^1 + d\mathbf{z}_1^0)/2$, $d\mathbf{z}_1^{\mathrm{b}} = (d\mathbf{z}_1^0 + d\mathbf{z}_0^{-1})/2$, and $d\mathbf{z}_\ell^1 = (d\mathbf{z}_0^{-1} + d\mathbf{z}_{-1}^0)/2$, leading to

$$\begin{aligned}
&\frac{1}{8\Delta t}\left((d\mathbf{z}_0^1 + d\mathbf{z}_{-1}^0) \wedge K(d\mathbf{z}_0^1 + d\mathbf{z}_{-1}^0) + (d\mathbf{z}_0^1 + d\mathbf{z}_1^0) \wedge K(d\mathbf{z}_0^1 + d\mathbf{z}_1^0)\right. \\
&\qquad \left. -(d\mathbf{z}_0^{-1} + d\mathbf{z}_{-1}^0) \wedge K(d\mathbf{z}_0^{-1} + d\mathbf{z}_{-1}^0) - (d\mathbf{z}_1^0 + d\mathbf{z}_0^{-1}) \wedge K(d\mathbf{z}_1^0 + d\mathbf{z}_0^{-1})\right) \\
&+\frac{1}{8\Delta x}\left((d\mathbf{z}_0^1 + d\mathbf{z}_1^0) \wedge L(d\mathbf{z}_0^1 + d\mathbf{z}_1^0) + (d\mathbf{z}_1^0 + d\mathbf{z}_0^{-1}) \wedge L(d\mathbf{z}_1^0 + d\mathbf{z}_0^{-1})\right. \\
&\qquad \left. -(d\mathbf{z}_0^1 + d\mathbf{z}_{-1}^0) \wedge L(d\mathbf{z}_0^1 + d\mathbf{z}_{-1}^0) - (d\mathbf{z}_0^{-1} + d\mathbf{z}_{-1}^0) \wedge L(d\mathbf{z}_0^{-1} + d\mathbf{z}_{-1}^0)\right) = 0,
\end{aligned}$$

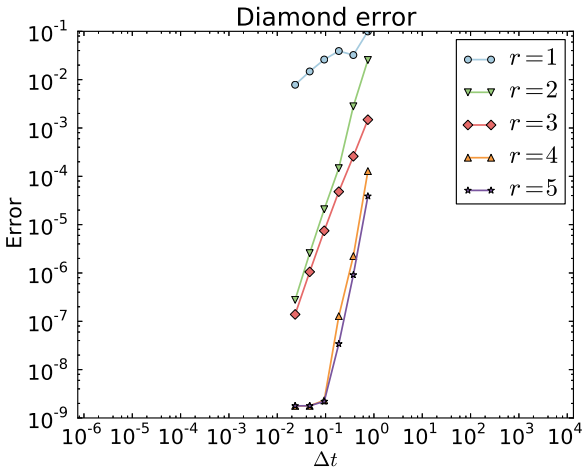

FIG. 8. *The error of the diamond scheme with varying r applied to the multisymplectic Hamiltonian PDE arising from the Sine–Gordon equation. The true solution was the so-called breather on the domain $[-30, 30]$. The Courant number is fixed at $\frac{1}{2}$ as Δt is decreased. The order of the method appears to be r when r odd and $r+1$ when r even (see text).*

which upon expanding and simplifying leads to the simple diamond scheme conservation law given in Proposition 2. ∎

Numerical test of diamond scheme. The diamond scheme with varying r was used to solve the Sine–Gordon equation as in section 2. The exact solution is the so-called breather given in (2.9), and the error is the discrete 2-norm of u given in (2.10). The number of diamonds at each time level is $N = 40, 80, \ldots, 1280$, and the integration time, $T = 1.5$, is twice the largest time step. The Courant number $\frac{\Delta t}{\Delta x} = \frac{1}{2}$ is held fixed. The $2rN$ initial values of $z = (u, u_t, u_x)$ needed at the bottom edge of the first row of diamonds are provided by the exact solution. The results for the global error are shown in Figure 8. It is apparent that for this problem, the order appears to be r when r is odd and $r+1$ when r is even. The superconvergence property of the underlying Gauss Runge–Kutta method, which has order $2r$, has been lost. But this is expected, since the underlying scheme has superconvergence on the end points, not at the internal stages where it has order $r+1$. It is these internal stages, the diamond edge points, that the diamond scheme operates on.

4. Dispersion analysis.

LEMMA 7. *For the linear multi-Hamiltonian*

$$K\mathbf{z}_t + L\mathbf{z}_x = S\mathbf{z}, \tag{4.1}$$

where S is a constant $n \times n$ real symmetric matrix, the dispersion relation between the wave number $\xi \in \mathbb{R}$ and frequency $\omega \in \mathbb{R}$ is given by

$$p(\xi, \omega) = \det(-i\omega K + i\xi L - S) = 0.$$

Proof. Assume $\mathbf{z} = e^{i(\xi x - \omega t)}\mathbf{c}$, where $\mathbf{c}$ is a constant vector, is a solution to (4.1). Substitution yields

$$(-i\omega K + i\xi L - S)\mathbf{c} = 0.$$

For nontrivial solutions the matrix on the left must have zero determinant. ∎

If there are any solutions to $p(\omega,\xi)=0$ with ξ real and ω complex but not real, then the PDE has solutions that grow without bound. For example, the dispersion relation for the wave equation, $u_{tt}-u_{xx}=0$, is $p(\xi,\omega)=\omega(\omega^2-\xi^2)=0$, so all solutions are bounded. For the equation $u_{tt}+u_{xx}=0$, the dispersion relation is $p(\xi,\omega)=\omega(\omega^2+\xi^2)=0$, so there are unbounded solutions.

THEOREM 8. *The simple diamond scheme applied to the linear multi-Hamiltonian equation has the dispersion relation between $\mathcal{X}\Delta x,\Omega\Delta t\in[-\pi,\pi]$ defined by*

$$P(\mathcal{X}\Delta x,\Omega\Delta t)=p(h(\mathcal{X}\Delta x,\Omega\Delta t))=p(h_1(\mathcal{X}\Delta x,\Omega\Delta t),h_2(\mathcal{X}\Delta x,\Omega\Delta t))=0,$$

where p is given in Lemma 7 and

$$\begin{aligned} h(x,y)&=(h_1(x,y),h_2(x,y)),\\ h_1(x,y)&=\frac{4\sin\left(\frac{1}{2}x\right)}{\Delta x\left(\cos\left(\frac{1}{2}x\right)+\cos\left(\frac{1}{2}y\right)\right)},\\ h_2(x,y)&=\frac{4\sin\left(\frac{1}{2}y\right)}{\Delta t\left(\cos\left(\frac{1}{2}x\right)+\cos\left(\frac{1}{2}y\right)\right)}. \end{aligned} \tag{4.2}$$

Proof. Assume that a solution to the simple diamond scheme given in (2.1) is $\mathbf{z}_j^n=e^{i(\mathcal{X}j\Delta x-\Omega n\Delta t)}\mathbf{c}$, where $\mathbf{c}$ is a constant vector, and because adding a multiple of 2π to either of $\Omega\Delta t$ or $\mathcal{X}\Delta x$ does not change $\mathbf{z}_j^n$ they are restricted to $[-\pi,\pi]$. Substitution into (2.1) yields

$$\begin{aligned} &\left[\frac{1}{\Delta t}\left(e^{-i\Omega\frac{1}{2}\Delta t}-e^{i\Omega\frac{1}{2}\Delta t}\right)K+\frac{1}{\Delta x}\left(e^{i\mathcal{X}\frac{1}{2}\Delta x}-e^{-i\Omega\frac{1}{2}\Delta x}\right)L-\right.\\ &\qquad\left.\Rightarrow\ \frac{1}{4}S\left(e^{-i\Omega\frac{1}{2}\Delta t}+e^{i\Omega\frac{1}{2}\Delta t}+e^{i\mathcal{X}\frac{1}{2}\Delta x}+e^{-i\mathcal{X}\frac{1}{2}\Delta x}\right)\right]\mathbf{c}=0\\ \Rightarrow&\left[\frac{-2i}{\Delta t}\sin\left(\tfrac{1}{2}\Omega\Delta t\right)K+\frac{2i}{\Delta x}\sin\left(\tfrac{1}{2}\mathcal{X}\Delta x\right)L-\frac{S}{2}\left(\cos\left(\tfrac{1}{2}\Omega\Delta t\right)+\cos\left(\tfrac{1}{2}\mathcal{X}\Delta x\right)\right)\right]\mathbf{c}=0\\ \Rightarrow&\left[\frac{-4i\sin\left(\frac{1}{2}\Omega\Delta t\right)K}{\Delta t\left(\cos\left(\frac{1}{2}\Omega\Delta t\right)+\cos\left(\frac{1}{2}\mathcal{X}\Delta x\right)\right)}+\frac{4i\sin\left(\frac{1}{2}\mathcal{X}\Delta x\right)L}{\Delta x\left(\cos\left(\frac{1}{2}\Omega\Delta t\right)+\cos\left(\frac{1}{2}\mathcal{X}\Delta x\right)\right)}-S\right]\mathbf{c}=0\\ &\qquad\Rightarrow\left[-ih_2(\mathcal{X}\Delta x,\Omega\Delta t)K+ih_1(\mathcal{X}\Delta x,\Omega\Delta t)L-S\right]\mathbf{c}=0. \end{aligned}$$

For nontrivial solutions the matrix on the left must have zero determinant, so $p(h_1(\mathcal{X}\Delta x,\Omega\Delta t),h_2(\mathcal{X}\Delta x,\Omega\Delta t))=0$. ∎

LEMMA 9. *The $r=1$ diamond scheme applied to the linear multi-Hamiltonian equation has a dispersion relation between $\tilde{\Omega},\tilde{\mathcal{X}}\in[-\pi,\pi]$ defined by*

$$\tilde{P}(\tilde{\mathcal{X}},\tilde{\Omega})=\det\left(-i2\tan\left(\frac{\tilde{\Omega}}{2}\right)\tilde{K}+i2\tan\left(\frac{\tilde{\mathcal{X}}}{2}\right)\tilde{L}-S\right)=0.$$

The tildes are reminders that this dispersion relation is in the $(\tilde{x},\tilde{t})$ coordinates.

Proof. Assume that a solution to the $r=1$ diamond scheme given in (3.5)–(3.9) is

$$\tilde{\mathbf{z}}_{\tilde{j}}^{\tilde{n}}=e^{i(\tilde{\mathcal{X}}\tilde{j}-\tilde{\Omega}\tilde{n})}\mathbf{c},$$

where $\tilde{\Omega}$ and $\tilde{\mathcal{X}}$ can be restricted to $[-\pi,\pi]$, and $\mathbf{c}$ is a constant vector. Note that in $(\tilde{x},\tilde{t})$ coordinates $\Delta x = \Delta t = 1$. Substitution into (3.5)–(3.9) (or (3.17) because $r=1$) yields after some simplification

$$\frac{\tilde{K}}{2}\left(e^{-i\tilde{\Omega}} + e^{i(\tilde{\mathcal{X}}-\tilde{\Omega})} - 1 - e^{i\tilde{\mathcal{X}}}\right)\mathbf{c} + \frac{\tilde{L}}{2}\left(e^{i\tilde{\mathcal{X}}} + e^{i(\tilde{\mathcal{X}}-\tilde{\Omega})} - 1 - e^{-i\tilde{\Omega}}\right)\mathbf{c} = \frac{S}{4}\left(1 + e^{i\tilde{\mathcal{X}}} + e^{-i\tilde{\Omega}} + e^{i(\tilde{\mathcal{X}}-\tilde{\Omega})}\right)\mathbf{c}.$$

The result follows after some simplification and using $\tan(x) = \frac{i(1-e^{2ix})}{1+e^{2ix}}$. ∎

Recall Theorem 5: modulo initial conditions, the $r=1$ diamond scheme and simple diamond scheme are equivalent. The following theorem shows that instead of directly calculating the dispersion relation for the $r=1$ diamond scheme, the dispersion relation from the simple diamond scheme can simply be transformed from (x,t) coordinates to $(\tilde{x},\tilde{t})$ coordinates.

THEOREM 10. *The simple and the $r=1$ diamond schemes have identical dispersion relations, that is, $\tilde{P}(\tilde{\mathcal{X}},\tilde{\Omega}) = P(\mathcal{X},\Omega)$.*

Proof.

$$\begin{aligned}
\mathbf{z}_j^n &= \tilde{\mathbf{z}}_{\tilde{j}}^{\tilde{n}} \\
\Rightarrow e^{i(\mathcal{X} j\Delta x - \Omega n\Delta t)}\mathbf{c} &= e^{i(\tilde{\mathcal{X}}\tilde{j} - \tilde{\Omega}\tilde{n})}\mathbf{c} \\
\Rightarrow e^{i(\mathcal{X}x - \Omega t)}\mathbf{c} &= e^{i(\tilde{\mathcal{X}}\tilde{x} - \tilde{\Omega}\tilde{t})}\mathbf{c} \\
\Rightarrow e^{i(\mathcal{X}\frac{\Delta x(\tilde{x}-\tilde{t})}{2} - \Omega\frac{\Delta t(\tilde{t}+\tilde{x})}{2})}\mathbf{c} &= e^{i(\tilde{\mathcal{X}}\tilde{x} - \tilde{\Omega}\tilde{t})}\mathbf{c} \qquad \text{using (3.1)} \\
\Rightarrow e^{i(\frac{\Delta x\mathcal{X} - \Omega\Delta t}{2}\tilde{x} - \frac{\Delta x\mathcal{X} + \Omega\Delta t}{2}\tilde{t})}\mathbf{c} &= e^{i(\tilde{\mathcal{X}}\tilde{x} - \tilde{\Omega}\tilde{t})}\mathbf{c},
\end{aligned}$$

thus

$$\tilde{\mathcal{X}} = \tfrac{\Delta x\mathcal{X} - \Omega\Delta t}{2} \quad \text{and} \quad \tilde{\Omega} = \tfrac{\Delta x\mathcal{X} + \Omega\Delta t}{2}. \tag{4.3}$$

Now

$$\begin{aligned}
&-i2\tan\left(\tfrac{\tilde{\Omega}}{2}\right)\tilde{K} + i2\tan\left(\tfrac{\tilde{\mathcal{X}}}{2}\right)\tilde{L} - S \\
&\quad= -i2\tan\left(\tfrac{\Delta x\mathcal{X}+\Omega\Delta t}{4}\right)\tilde{K} + i2\tan\left(\tfrac{\Delta x\mathcal{X}-\Omega\Delta t}{4}\right)\tilde{L} - S \\
&\quad= -i2\tan\left(\tfrac{\Delta x\mathcal{X}+\Omega\Delta t}{4}\right)\left(\tfrac{1}{\Delta t}K - \tfrac{1}{\Delta x}L\right) + i2\tan\left(\tfrac{\Delta x\mathcal{X}-\Omega\Delta t}{4}\right)\left(\tfrac{1}{\Delta t}K + \tfrac{1}{\Delta x}L\right) - S \\
&\quad= -i\frac{2}{\Delta t}\left(\tan\left(\tfrac{\Delta x\mathcal{X}+\Omega\Delta t}{4}\right) - \tan\left(\tfrac{\Delta x\mathcal{X}-\Omega\Delta t}{4}\right)\right)K \\
&\qquad + i\frac{2}{\Delta x}\left(\tan\left(\tfrac{\Delta x\mathcal{X}-\Omega\Delta t}{4}\right) + \tan\left(\tfrac{\Delta x\mathcal{X}+\Omega\Delta t}{4}\right)\right)L - S \\
&\quad= -i\frac{2}{\Delta t}\frac{2\sin\left(\frac{\Delta t\Omega}{2}\right)}{\cos\left(\frac{\Delta x\mathcal{X}}{2}\right) + \cos\left(\frac{\Delta t\Omega}{2}\right)}K + i\frac{2}{\Delta x}\frac{2\sin\left(\frac{\Delta x\mathcal{X}}{2}\right)}{\cos\left(\frac{\Delta x\mathcal{X}}{2}\right) + \cos\left(\frac{\Delta t\Omega}{2}\right)}L - S
\end{aligned}$$

using (4.3), (3.4), and (in the last step) $\tan(\frac{a+b}{2}) = \frac{\sin(a)+\sin(b)}{\cos(a)+\cos(b)}$. ∎

LEMMA 11. *Let $U = (-\pi,\pi)\times(-\pi,\pi)$ and let $V = h(U)$, where h is defined in (4.2). The map $h\colon U \to V$ is a diffeomorphism.*

Proof. The Jacobian of (h_1,h_2) is

$$J = \frac{2}{\Delta t\left(\cos(\frac{x}{2}) + \cos(\frac{y}{2})\right)^2}\begin{pmatrix} \lambda(1+\cos(\frac{x}{2})\cos(\frac{y}{2})) & \lambda\sin(\frac{x}{2})\sin(\frac{y}{2}) \\ \sin(\frac{x}{2})\sin(\frac{y}{2}) & (1+\cos(\frac{x}{2})\cos(\frac{y}{2}))\end{pmatrix},$$

where λ is the Courant number. By definition h is surjective, and it is straightforward to show that $\det(J) \neq 0$ for all $x, y \in U$. Thus J is a bijection and h is a local diffeomorphism. Because both U and V are connected open subsets of $\mathbb{R}^2$, V is simply connected, and because h is proper, h is a diffeomorphism. ∎

The discrete dispersion relation determined in Theorem 8 allows the linear stability of the method to be determined for any PDE for which the continuous dispersion relation is known. We illustrate this for the linear wave equation.

THEOREM 12. *The simple diamond scheme applied to the wave equation is linearly stable when* $\lambda = \frac{\Delta t}{\Delta x} \leq 1$.

Proof. It must be shown that for all $\mathcal{X}\Delta x \in [-\pi, \pi]$ there exists $\Omega\Delta t \in [-\pi, \pi]$ such that $P(\mathcal{X}\Delta x, \Omega\Delta t) = 0$, where, from Theorem 8, $P(x, y) = p(h(x, y)) = p(h_1(x, y), h_2(x, y))$, and for the wave equation $p(\xi, \omega) = \xi^2 - \omega^2$. We have

$$\begin{aligned} & P(\mathcal{X}\Delta x, \Omega\Delta t) = 0 \\ \Leftrightarrow\ & p(h_1(\mathcal{X}\Delta x, \Omega\Delta t), h_2(\Delta x, \Omega\Delta t)) = 0 \\ \Leftrightarrow\ & h_1(\mathcal{X}\Delta x, \Omega\Delta t) \pm h_2(\Delta x, \Omega\Delta t) = 0 \\ \Leftrightarrow\ & \frac{\sin(\frac{1}{2}\Omega\Delta t)}{\sin(\frac{1}{2}\mathcal{X}\Delta x)} = \frac{\Delta t}{\Delta x} \\ \Leftrightarrow\ & \Omega\Delta t = 2\sin^{-1}\left(\lambda \sin(\tfrac{1}{2}\mathcal{X}\Delta x)\right). \end{aligned} \tag{4.4}$$

When $\lambda \leq 1$ the right-hand side can be evaluated for all $\mathcal{X}\Delta x \in [-\pi, \pi]$ and gives $\Omega\Delta t \in [-\pi, \pi]$. ∎

Note that the dispersion relation of the simple box scheme for the linear wave equation, given in (4.4), is the same as that of the explicit 5-point method.

Another approach will now be illustrated. The condition that for all $x \in [-\pi, \pi]$ there exists $y \in [-\pi, \pi]$ such that $p(h(x, y)) = 0$ is equivalent to stating that $h\colon \mathbb{R} \times [-\pi, \pi]$ contains the solution to $p(\xi, \omega) = 0$. By Lemma 11 h is a diffeomorphism; thus the solution to $p(\xi, \omega) = 0$ only has to be between the boundaries $h(x, \pm\pi)$:

$$h(x, \pm\pi) = (h_1(x, \pm\pi), h_2(x, \pm\pi)) = \left(\frac{4\sin(x/2)}{\Delta x \cos(x/2)}, \pm\frac{4}{\Delta t \cos(x/2)}\right).$$

Let $\xi = h_1(x, y)$ and $\omega = h_2(x, y)$, and use the formula for $\cos\tan^{-1}$ to find

$$\omega = \pm\frac{4}{\Delta t}\sqrt{1 + \left(\frac{\Delta x \xi}{4}\right)^2}.$$

Thus the simple diamond scheme is stable for the wave equation iff

$$\xi \leq \pm\frac{4}{\Delta t}\sqrt{1 + \left(\frac{\Delta x \xi}{4}\right)^2}.$$

It is straightforward to check this holds iff $\lambda \leq 1$. Figure 9 illustrates the action of h and the linear wave equation dispersion relation. Figure 10 is similar except for the dispersion relation $p(\xi, \omega) = \omega - \xi + \xi^3$.

5. Discussion. Many features of the diamond scheme can be seen immediately from its definition:

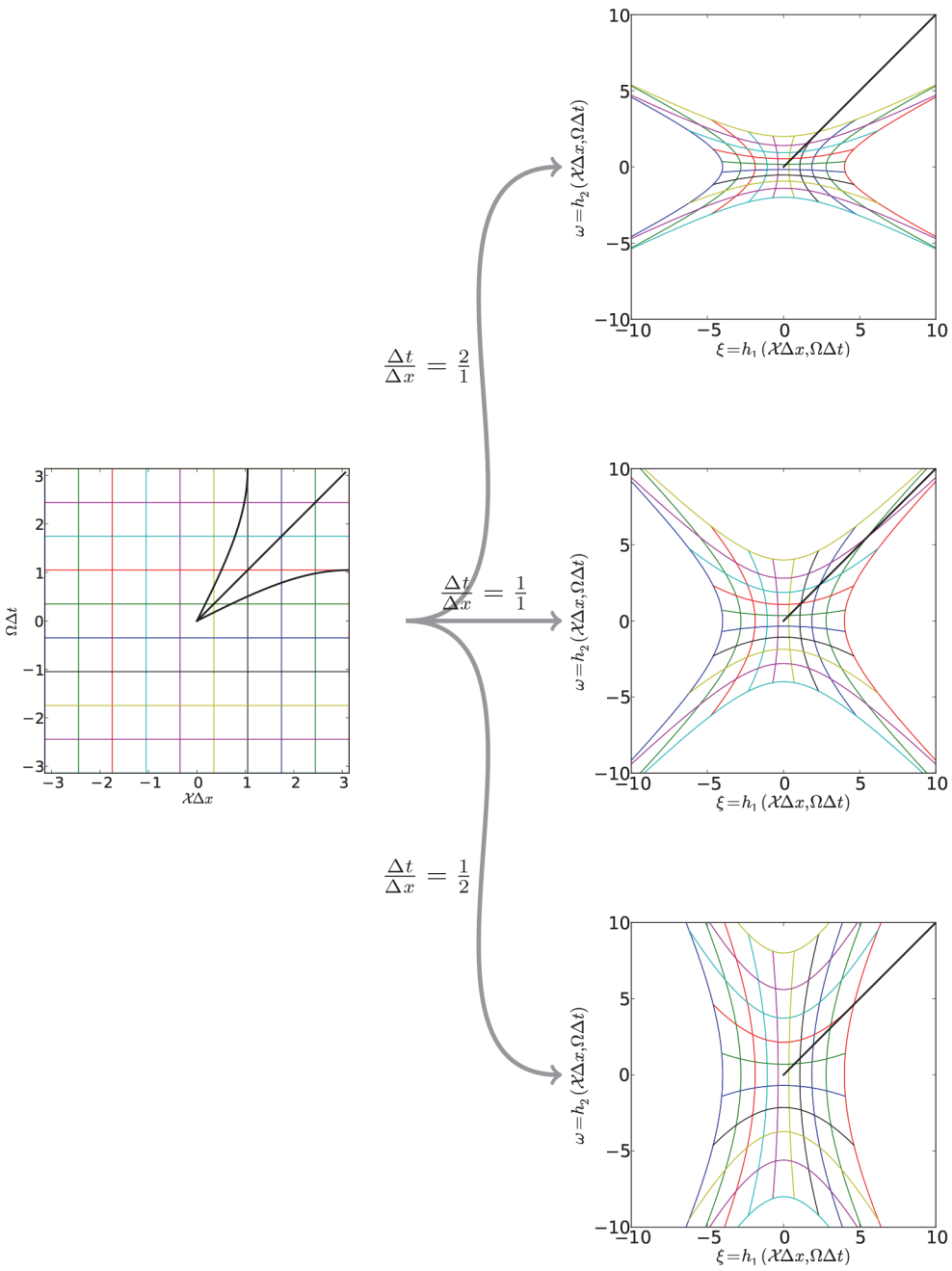

FIG. 9. *The domain* $(-\pi, \pi) \times (-\pi, \pi)$ *and three images under the map* $h = (h_1, h_2)$ *(equation* (4.2)*) with varying Courant number. The coordinates in the image space are* $(\xi, \omega) = (h_1(\mathcal{X}\Delta x, \Omega\Delta t), h_2(\mathcal{X}\Delta x, \Omega\Delta t))$. *A portion of the wave equation dispersion relation* $p(\xi, \omega) = \omega - \xi$ *is displayed, and the discrete dispersion relations, obtained by applying* h^{-1}, *are shown on the left. When* $\lambda = 2$ *the discrete dispersion relation has no real solution for* $\mathcal{X}\Delta x > 1$, *thus the simple diamond scheme is unstable.*

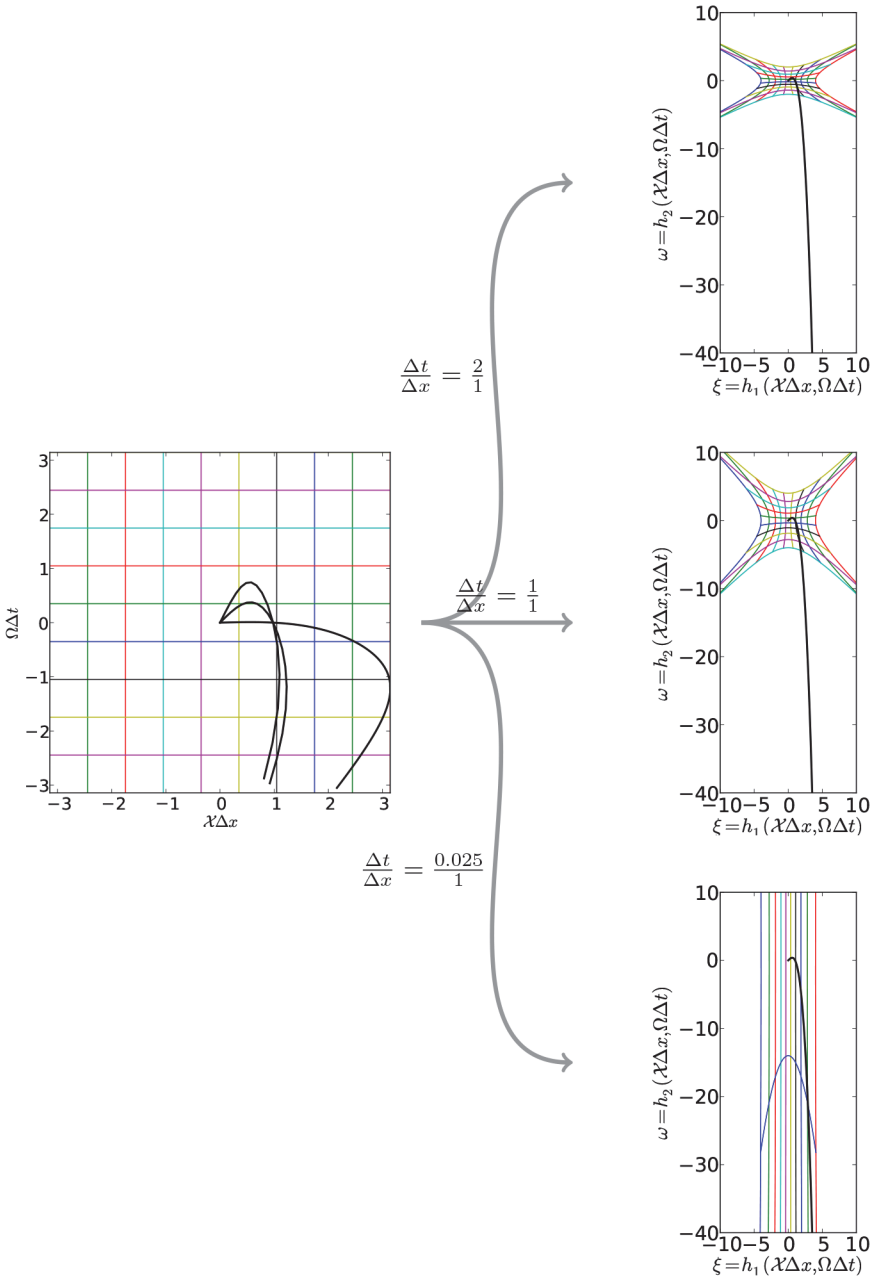

FIG. 10. *The domain* $(-\pi, \pi) \times (-\pi, \pi)$ *and three images under the map* $h = (h_1, h_2)$ *(equation* (4.2)*) with varying Courant number. The coordinates in the image space are* $(\xi, \omega) = (h_1(\mathcal{X}\Delta x, \Omega\Delta t), h_2(\mathcal{X}\Delta x, \Omega\Delta t))$. *A portion of the dispersion relation* $p(\xi, \omega) = \omega - \xi + \xi^3$ *is displayed, and the discrete dispersion relations, obtained by applying* h^{-1}, *are shown on the left. When* $\lambda \gtrapprox 0.025$ *the discrete dispersion relation doesn't have a real solution for all* $\mathcal{X}\Delta x > 0$, *and thus the simple diamond scheme is unstable.*

1. It is defined for all multi-Hamiltonian systems (1.1).
2. It is only locally implicit within each diamond. Such locality is suitable for hyperbolic systems with finite wave speeds. Compared to fully implicit schemes like Runge–Kutta box schemes, this leads to
   (a) nonlinear equations that have a solution;
   (b) faster nonlinear solves;
   (c) better parallelization, as no communication between diamonds is required during solves and all diamonds can be solved in parallel—initial experiments indicate that the scheme scales well with the number of processors; and
   (d) local treatment of boundary conditions—ad hoc schemes for particular multi-Hamiltonian equations and boundary conditions have been found.

   On the other hand, the implicitness within a diamond should improve stability compared to fully explicit methods in cases where $S(z)$ contributes (a moderate amount of) stiffness to the equation.
3. It is linear in z; this is expected to lead to
   (a) preservation of conservation laws associated with linear symmetries;
   (b) better transmission of waves at mesh boundaries, as has been found for the (linear) simple box scheme [9]; and
   (c) easier handing of dispersion relations, which can be determined once and for all for *all* multi-Hamiltonian PDEs, as in Theorem 8.

   It is the linearity of the method that means it can capture part of the continuous dispersion relation via a smooth remapping of frequencies.

This combination of properties, together with its expected and observed high-order, is new for multisymplectic integrators.

At the same time, the novel mesh introduces some complications:

1. The implementation is slightly more involved than on a standard mesh; in practice we have not found this to be significant. The parallel implementation is generally easier than on a standard mesh.
2. The interaction of the mesh with the boundaries means that they need special treatment (but at least they *can* be treated).
3. The mesh geometry introduces some distortions to the dispersion relation, which is illustrated in Figures 9 and 10.

The principle of the diamond method is extremely general and can be applied to a very wide range of PDEs; it may have applications beyond the multisymplectic PDE (1.1). It extends easily to $2d$-hedral meshes for PDEs in d-dimensional space-time, again subject to the CFL condition. However, at present, to prove existence of solutions of the nonlinear equations we need to restrict ourselves to a particular class of equations; ideally one would like to establish existence of numerical solutions for all PDEs (1.1) and relate them to the existence of solutions to the PDE itself.

In future work we shall address these issues, develop initialization and boundary schemes, and establish the order of the diamond scheme.

Acknowledgments. We would like to thank Reinout Quispel for bringing the staircase method to our attention and Stephen Marsland for useful discussions.

REFERENCES

[1] U. Ascher and R. McLachlan, *On symplectic and multisymplectic schemes for the KdV equation*, J. Sci. Comput., 25 (2005), pp. 83–104.

[2] U. M. Ascher and R. I. McLachlan, *Multisymplectic box schemes and the Korteweg–de Vries equation*, Appl. Numer. Math., 48 (2004), pp. 255–269.

[3] T. J. Bridges and S. Reich, *Multi-symplectic integrators: numerical schemes for Hamiltonian PDEs that conserve symplecticity*, Phys. Lett. A, 284 (2001), pp. 184–193.
[4] T. J. Bridges and S. Reich, *Numerical methods for Hamiltonian PDEs*, J. Phys. A, 39 (2006), pp. 5287–5320.
[5] E. Celledoni, V. Grimm, R. I. McLachlan, D. McLaren, D. O'Neale, B. Owren, and G. Quispel, *Preserving energy resp. dissipation in numerical PDEs using the "average vector field" method*, J. Comput. Phys., 231 (2012), pp. 6770–6789.
[6] J.-B. Chen, M.-Z. Qin, and Y.-F. Tang, *Symplectic and multi-symplectic methods for the nonlinear Schrödinger equation*, Comput. Math. Appl., 43 (2002), pp. 1095–1106.
[7] G. Cohen, *Higher-Order Numerical Methods for Transient Wave Equations*, Springer, New York, 2002.
[8] J. Frank, B. E. Moore, and S. Reich, *Linear PDEs and numerical methods that preserve a multisymplectic conservation law*, SIAM J. Sci. Comput., 28 (2006), pp. 260–277.
[9] J. Frank and S. Reich, *On Spurious Reflections, Nonuniform Grids and Finite Difference Discretizations of Wave Equations*, CWI Report MAS-E0406, Center for Mathematics and Computer Science, 2004.
[10] J. Hong and C. Li, *Multi-symplectic Runge–Kutta methods for nonlinear Dirac equations*, J. Comput. Phys., 211 (2006), pp. 448–472.
[11] J. Hong, Y. Liu, H. Munthe-Kaas, and A. Zanna, *Globally conservative properties and error estimation of a multi-symplectic scheme for Schrödinger equations with variable coefficients*, Appl. Numer. Math., 56 (2006), pp. 814–843.
[12] A. Islas, D. Karpeev, and C. Schober, *Geometric integrators for the nonlinear Schrödinger equation*, J. Comput. Phys., 173 (2001), pp. 116–148.
[13] A. Islas and C. Schober, *On the preservation of phase space structure under multisymplectic discretization*, J. Comput. Phys., 197 (2004), pp. 585–609.
[14] C. Jia-Xiang, Y. Bin, and L. Hua, *Multisymplectic implicit and explicit methods for Klein–Gordon–Schrödinger equations*, Chinese Physics B, 22 (2013), 030209.
[15] L. Kong, L. Wang, S. Jiang, and Y. Duan, *Multisymplectic Fourier pseudo-spectral integrators for Klein–Gordon–Schrödinger equations*, Sci. China Math., 56 (2013), pp. 915–932.
[16] B. Leimkuhler and S. Reich, *Simulating Hamiltonian Dynamics*, Cambridge Monogr. Appl. Comput. Math., Cambridge University Press, Cambridge, UK, 2004.
[17] C. Liao and X. Ding, *Nonstandard finite difference variational integrators for nonlinear Schrödinger equation with variable coefficients*, Adv. Difference Equation, 2013 (2013), pp. 1–22.
[18] R. McLachlan, Y. Sun, and P. Tse, *Linear stability of partitioned Runge–Kutta methods*, SIAM J. Numer. Anal., 49 (2011), pp. 232–263.
[19] R. I. McLachlan and D. R. J. O'Neale, *Preservation and destruction of periodic orbits by symplectic integrators*, Numer. Algorithms, 53 (2010), pp. 343–362.
[20] R. I. McLachlan, Y. Sun, and B. Ryland, *High order multisymplectic Runge–Kutta methods*, SIAM J. Sci. Comput., 36 (2014), pp. A2199–A2226.
[21] B. E. Moore and S. Reich, *Multi-symplectic integration methods for Hamiltonian PDEs*, Future Generation Computer Systems, 19 (2003), pp. 395–402.
[22] S. Reich, *Multi-symplectic Runge–Kutta collocation methods for Hamiltonian wave equations*, J. Comput. Phys., 157 (2000), pp. 473–499.
[23] B. Ryland, *Multisymplectic Integration*, Ph.D. thesis, Massey University, New Zealand, 2007.
[24] B. N. Ryland and R. I. McLachlan, *On multisymplecticity of partitioned Runge–Kutta methods*, SIAM J. Sci. Comput., 30 (2008), pp. 1318–1340.
[25] B. N. Ryland, R. I. Mclachlan, and J. Frank, *On the multisymplecticity of partitioned Runge–Kutta and splitting methods*, Int. J. Comput. Math., 84 (2007), pp. 847–869.
[26] J. Simo and N. Tarnow, *The discrete energy-momentum method. Conserving algorithms for nonlinear elastodynamics*, Z. Angew. Math. Phys., 43 (1992), pp. 757–792.
[27] J.-Q. Sun and M.-Z. Qin, *Multi-symplectic methods for the coupled 1D nonlinear Schrödinger system*, Comput. Phys. Comm., 155 (2003), pp. 221–235.
[28] P. H. van der Kamp and G. Quispel, *The staircase method: Integrals for periodic reductions of integrable lattice equations*, J. Phys. A, 43 (2010), 465207.
[29] J.-J. Wang and L.-T. Wang, *Multi-symplectic Preissmann scheme for a high-order wave equation of KdV type*, Appl. Math. Comput., 219 (2013), pp. 4400–4409.
[30] P. F. Zhao and M. Z. Qin, *Multisymplectic geometry and multisymplectic Preissmann scheme for the KdV equation*, J. Phys. A, 33 (2000), pp. 3613–3626.
[31] Z.-Q. Lv, Y.-S. Wang, and Y.-Z. Song, *A new multi-symplectic integration method for the nonlinear Schrödinger equation*, Chinese Physics Letters, 30 (2013), 030201.